



Investigating the Impact of Methanol Concentration and Implementation of a Coefficient Diagram-Based Control System for Direct Methanol Fuel Cell Operation

Ramasamy Govindarasu¹ · Divya Baskaran^{2,4} · Solaiappan Somasundaram³ · Hun-Soo Byun²

Received: 19 March 2024 / Revised: 7 April 2024 / Accepted: 12 April 2024 / Published online: 21 April 2024
© The Author(s), under exclusive licence to Korean Institute of Chemical Engineers, Seoul, Korea 2024

Abstract

The impact of methanol concentration on direct methanol fuel cell (DMFC) of 45 cm² zones of activity was experimentally studied with serpentine channel field design. The performance of the DMFC was analyzed and the optimum methanol concentration was determined with a polarization curve. A recently suggested Coefficient Diagram derived from PI Controller (CD-PIC) was used to run the model-based DMFC in a closed loop with the manipulated variable as methanol concentration. The CD-PIC design is simple and efficient compared to the Bode Diagram-based controller design. It is also used to test the performance and robustness of the system apart from the stability. A recently suggested PI Controller that relies on a Coefficient Schematic is employed in DMFC operation. The progress of the proposed CD-PIC is evaluated under load abandonment circumstances and set point monitoring. Set point tracking and load rejection tests are carried out with step changes at different operating points. The controller execution is evaluated in ways of controller progress measuring (CPM) indices. The suggested performance metrics for the proposed CD-PIC indicate that it yields better performance for servo problems and regulatory problems which support the supremacy of CD-PIC. The robustness of the CD-PIC is also analyzed. From the CPM indices, it is concluded that the recently created CD-PIC for DMFC is found as highly robust.

Keywords DMFC · Methanol concentration · CD-PIC · Stability · CPM indices · Robustness

Introduction

Life on Earth is now incredibly comfortable thanks to significant technological advancements, but this comfort also came with a burden: supplying and locating high-quality energy. The past decade has seen an exponential increase in

human population. These factors along with others, demand the necessary alternatives to the energy crisis. Fuel cells have emerged as an ideal solution to the recent severe energy crisis. Despite the development of several fuel cell types, researchers are still looking for the most promising fuel cell with the highest efficiency [1]. The optimum way of transforming chemical energy into electrical energy is the direct methanol fuel cell (DMFC). In the near future, direct alcohol fuel cells-of which DMFC is the leading type-are anticipated to supersede traditional proton-exchange membrane (PEM) fuel cells [2, 3]. The direct methanol fuel cell is fed with aqueous solution of methanol, unlike PEM fuel cells that are fed with hydrogen [4].

A liquid-type fuel cell is operated based on the hydrolysis of the fuel liquid into hydrogen on the anode side and continuously reform/oxidize to produce water and carbon dioxide on the cathode side [5]. Many attractive liquid fuels were proposed and researched such as formic acid, ethanol, methanol, methoxymethanes, methyl formate, etc. The combustion of methanol to CO₂ and water plays major attention due to the benefit of clean combustion to CO₂. The

✉ Ramasamy Govindarasu
rgovind@svce.ac.in

✉ Hun-Soo Byun
hsbyun@jnu.ac.kr

¹ Department of Chemical Engineering, Sri Venkateswara College of Engineering, Sriperumbudur 602117, India

² Department of Chemical and Biomolecular Engineering, Chonnam National University, Yeosu, Jeonnam 59626, South Korea

³ Alagappa Chettiar Government College of Engineering and Technology, Karaikudi 630004, India

⁴ Department of Biomaterials, Saveetha Dental College and Hospitals, Saveetha Institute of Medical and Technical Sciences, Chennai 600077, India

main advantage of DMFC is the hydrogen oxidation on the cathode side is significantly faster and performs better than direct hydrogen cells [6]. However, the intermediates are produced during methanol oxidation since the kinetics are inherently slower. Hence, the adsorbents are recommended for the adsorption of oxygen-containing intermediates. The development of sufficient electrode fabrication induces a better cell design and effective performance in small-cell DMFCs [7–9]. Higher efficiency fuel cells are not necessarily implied by the fuel cells' basic design. Enhancing fuel cell efficiency is mostly dependent on modeling and control.

To track the development of cell effectiveness [10, 11], a Laplace domain model of DMFC is created and is related to the control mechanism in various fields, it is imperative to design a reliable control system. Simple systems do not require the use of classical control design techniques. Therefore, the development of a reliable control system is necessary. Elementary systems use classical control design methodologies, but advanced systems do not. Advanced systems have been the focus of contemporary control development, yet controller layout and tuning are challenging. Limited reports are published on the design of controller for the DMFC. A maximum power point tracking (MPPT) control method for highly efficient direct methanol fuel cell generation systems via T–S fuzzy model is proposed by Ouyang et al. [12]. To alleviate fuel cell degradation during long-time operation an adaptive control strategy is developed by Yang et al. [13]. However, polynomial-based coefficient diagram method (CDM) is studied limited for the design of controller [14]. Hence, the polynomial-based coefficient diagram method is used to design controller for DMFC in the present work. CDM is a Pole placement method and it involves the concepts of classical and modern control techniques. Here both the plant and controller are represented by the numerator and denominator polynomials respectively, better results can be achieved against pole-zero cancellations. Considering the design specifications (settling time and overshoot), coefficients of the controller polynomials are found later. By utilizing the Coefficient Diagram, the performance of the controller can be predicted before implementing. The two-degree-of-freedom control system framework ensures minimal or no overshoot in the step response of the closed-loop system. Determining the settling time at the outset and organizing subsequent layout accordingly, and the system's ability to withstand abrupt changes [15].

With polynomial-based CDM, the layout methodology of DMFC is clear-cut, methodical, and practical. For time delay processes with various characteristics that call for several tuning techniques in traditional PI controller design, a single design procedure is employed. The Coefficient Diagram is a more precise and user-friendly tool when designing controllers [16, 17]. Chi et al. investigated the energy conversion efficiency during optimization of operating concentration

control for the effective operation of DMFC [18]. Govindarasu and Somasundaram studied the effect of cell temperature on the performance of direct methanol fuel cell [19]. Giordano et al. analyzed the effect of methanol concentration during operation of DMFC by using electrochemical spectroscopy, however, the effect of set point monitoring and load abandonment test is not reported [20]. The existing control strategies to control DMFC are conventional and analytical design oriented and time consuming to design/tuning controllers. The proposed control strategy is coefficient diagram (graphical design) based which are very simple and less time consuming for design of controller and tuning of controller with better results to meet the controller objectives.

Therefore, the present study aims to analyze and optimize methanol concentration in the newly designed coefficient diagram-based proportional integral controller in DMFC. The methanol concentration of 1 M, 2 M, and 3 M was studied with a peak power density which is important to the portable application. The characterization of the model-based controller was studied according to the set point monitoring and load abandonment test. Furthermore, the potential performance of the newly designed controller is compared with the conventional controller.

Materials and Methods

Operations of DMFC

The Direct Methanol Fuel Cell transfers the chemical power to electrical power directly with superior competence. A proton interchange membrane fuel cell subtype known as the DMFC is often supplied with an aqueous solution of methanol. At the location of the anode, aqueous methanol is introduced. It traverses the diffusion layer and enters the catalytic region where it undergoes electrochemical oxidation to generate protons, electrons, and carbon dioxide. The electrons generated are withdrawn as power through an outermost circuit. The protons generated during the oxidation process migrate through the Nafion-117 membrane to reach the cathode's catalytic layer. There, they play a crucial role in facilitating the reduction of oxygen to produce water on the cathode side. Figure 1 shows the schematic illustration of the process flow diagram of the DMFC. Figure 2 represents the experimental connection setup of the photo plate of DMFC [21].

Real-time experimental studies are carried out in DMFC (Fig. 3) for various methanol concentrations. The output (voltage) was noted at galvanostatic conditions. *I*–*V* Curve data from the experiential run are recorded for different concentrations of methanol viz. 1 M, 2 M, and 3 M with the cell temperature 333 K, 1 cm³ methanol flowrate, 1 cm³

Fig. 1 Schematic illustration of the process flow diagram of the DMFC

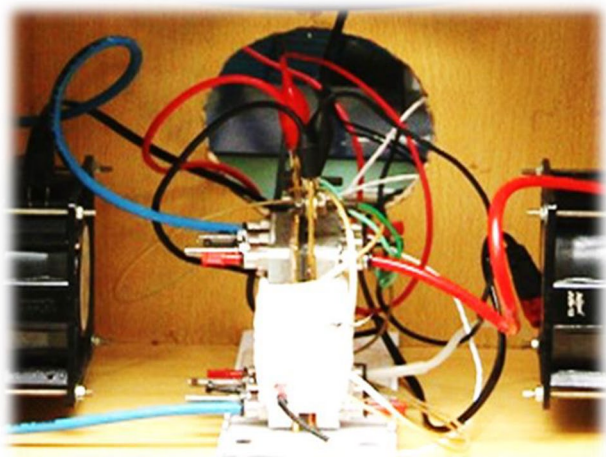
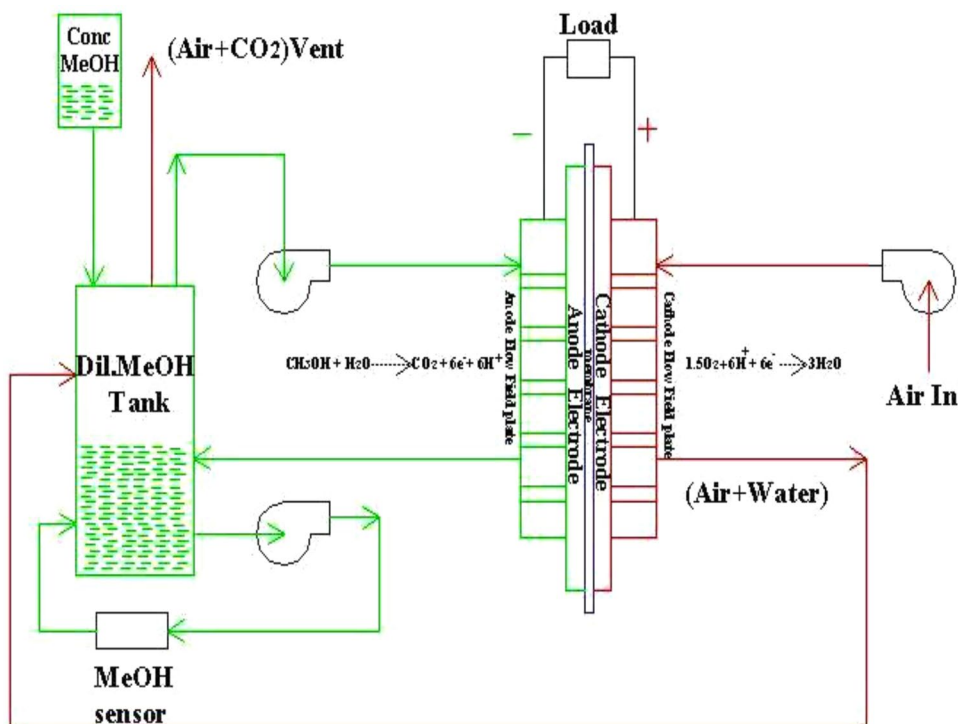


Fig. 2 Experimental connection setup of the DMFC photo plate

air flowrate, and 1 psi air pressure. It has been noted that the voltage at an open circuit is within the spectrum of 0.5–0.6 V.

Development of a Laplace Domain Model for DMFC

The First Order Plus Time Delay (FOPTD) model of DMFC is developed from the mathematical modeling created using the DMFC’s mathematical modeling expressions [10, 22]. The computation studies accompanied by the setpoint tracking ($\pm 10\%$ and $\pm 15\%$) at two distinct points of operation in



Fig. 3 Real-time laboratory experimental setup of DMFC control system

a state of stability (40% and 60% of the voltage within the cell.) are completed, and the results are documented. Following this feedback using the Sundaresan et al. model identification procedure [23], prototype parameters of the FOPTD system such as process gain, processing duration constant, and time delay are determined. With the most undesirable instance model identification technique, bigger process gain, longer process time delay, and decreased process time constant are regarded as the most important among these model

parameters to develop the Laplace domain transfer function model for DMFC [24, 25] and are represented as

$$G_p(s) = \frac{0.107}{18.0s + 1} e^{-2s} \tag{1}$$

Using Pade’s approximation technique, the delay in the existing DMFC transfer function model is calculated and expressed as $G_{p1}(s)$. When designing the CD-PI Controller, the DMFC’s approximated FOPTD model [26] is considered.

$$G_{p1}(s) = \frac{0.107 - 0.107s}{18s^2 + 19s + 1} \tag{2}$$

Cutting-Edge Materialization of CDM Controller

Figure 4 displays the block diagram of the CDM-based control system. The numerator and denominator polynomials of the plant’s transfer function are $N(s)$ and $D(s)$, respectively. The polynomial $A(s)$ represents the forward denominator of the controller transfer function, whilst the polynomials $F(s)$ and $B(s)$ represent the reference and feedback numerators, correspondingly. The controller’s transfer function mimics a two-degrees-of-freedom system structure [27, 28] since it contains two numerators.

The steady-state output of the system is given by

$$Y = \frac{N(s)F(s)}{P(s)}r + \frac{A(s)N(s)}{P(s)}d \tag{3}$$

where $P(s)$, which is characterized by the closed-loop system’s distinctive polynomial.

$$P(s) = A(s)D(s) + B(s)N(s) + \sum_{i=0}^n a_i s^i \tag{4}$$

where $A(s)$ and $B(s)$ are chosen as the control polynomial and selected just like

$$A(s) = \sum_{i=0}^p l_i s^i \text{ and } B(s) = \sum_{i=0}^q k_i s^i, p \geq q \text{ and } a_i > 0.$$

The closed loop reaction speed is indicated by the equivalent time constant (τ_{eq}), while the stability and time response pattern are shown by the values of the stability indices (γ_i). $\tau_s = t_s/2.5$, where t_s is the custom-built settling period. $\gamma_i = \{2.5, 2, 2, \dots, 2\}$. Using τ_{eq} and γ_i a desired characteristic polynomial ($P_{target}(s)$) is represented as

$$P_{target}(s) = a_0 \left[\sum_{i=2}^n \left(\prod_{j=1}^{i-1} \frac{1}{\gamma_{i-j}^j} \right) (\tau_{eq} s)^i \right] + \tau_s + 1 \tag{5}$$

Equating Eqs. 4 and 5, a diophantine equation of $A(s)D(s) + B(s)N(s) = P_{target}(s)$ is acquired. From this equation, the controller specifications (K_i, l_i) are computed. With these coefficients (K_i, l_i), the CDM controller polynomials $A(s), B(s)$, and closed-loop characteristic polynomial $P(s)$ are determined.

Proposed Coefficient Diagram Based PI Controller

In this work, a new CD-PI controller is designed for DMFC. The stability indices (γ_1, γ_2) are selected from the user defined stability indices as detailed in Sect. “Proposed Coefficient Diagram based PI Controller”. Equivalent CDM block diagram is obtained using the block diagram reduction rule [29, 30]. By selecting $F(s)$ in this way, the error that may occur in the steady-state response of the closed-loop system is reduced to zero.

The set-point filter element $F(s)$ and the CD-PIC polynomials are expressed as given below since the error that may occur in the steady-state response of the closed-loop system is reduced to zero.

$$F(s) = P(s)/N(s)|_{s=0} = P(0)/N(0) = 1/K = k_0 \tag{6}$$

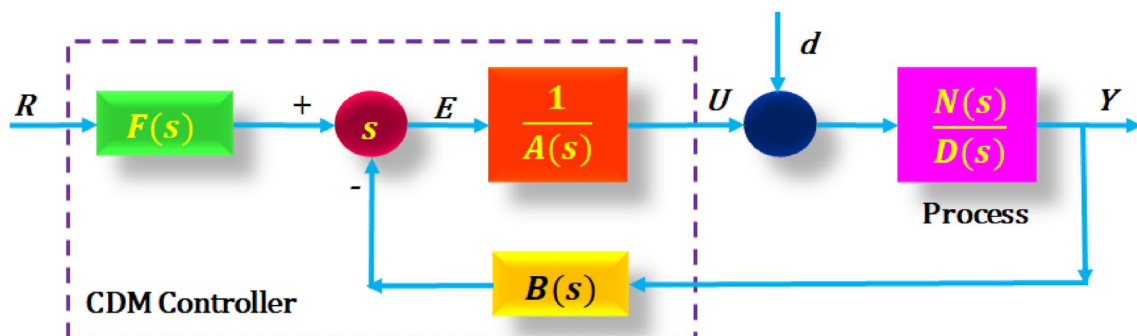


Fig. 4 Block diagram of the polynomial-based control system

$A(s)$ and $B(s)$ in Fig. 5 represented to $A(s) = s$; $B(s) = k_1s + k_0$.

The goal characteristic polynomial $P_{target}(s)$ and the closed loop characteristic polynomial $P(s)$ are found. The proposed CD-PIC system shown in Fig. 5a consists of the primary controller $C(s)$ and feed-forward controller $C_f(s)$. $C(s)$ is selected $C(s) = K_c \left(1 + \frac{1}{T_i s} \right)$ which is like trad its PI controller. By comparing Fig. 5a with Fig. 5b, the subsequent correlations are discovered.

$$\frac{B(s)}{A(s)} = K_c \left(1 + \frac{1}{T_i s} \right) \tag{7}$$

$$\frac{K_1s + K_0}{s} = K_c \left(1 + \frac{1}{T_i s} \right) \tag{8}$$

Parameters of polynomial CD-PIC are obtained by matching the terms' coefficients to the same power (where $K_c = k_1$ and $T_i = k_0/K_0$).

The parameters of $C_f(s)$ are directly obtained from the PI controller equation [31].

$$C_f(s) = \frac{F(s)}{B(s)} = \frac{k_0}{k_1s + k_0} = \frac{1}{T_i s + 1} \tag{9}$$

Selection of Stability Indices

Selection of stability indices γ_1 and γ_2 are of utmost importance during the design of CD-PIC with DMFC system,

since these indices ascertain the system's robustness and the closed loop step response's transient character Manabe guidelines are utilized to determine the CD-PI Controller variables for different combinations of γ_1, γ_2 values [32, 33]. CD-PI Controller parameters are calculated for different combinations of stability indices (γ_1, γ_2). The computed CD-PIC design parameters for different combinations of stability indices (γ_1, γ_2) are derived. At OP of 40% output voltage of DMFC, a simulation run is carried out for set point changes of + 10%. In this section, different combinations of γ_1 , and γ_2 are grouped as Group-I and Group-II. Servo response of CD-PIC for different combinations of stability indices (γ_1, γ_2) are studied.

Performance measures namely error indices and time domain indices are obtained from Fig. 6a and b and are summarized in Table 1.

It is evident from Fig. 6 and Table 1, that the response made by CD-PIC for γ_1 values namely 2, 3, and 4 are oscillatory, with a high percentage of overshoot and settling time. The error indices and time domain indices values for these responses are found to be high. But servo response with $\gamma_1 = 5$ gives minimum oscillations, lower settling time, no overshoot, and comparatively lower ISE, and IAE values. It is also observed from the said figures and table that the responses made by CD-PIC for different values of γ_2 Viz., 2, 3, 3.5, 4, and 5 are highly oscillatory with overshoot except that corresponding to $\gamma_2 = 2.5$. The error indices presented in Table 1 have minimum deviation for all values of γ_2 . However, it is noticed that the time domain indices have higher times of rising and settling for all γ_2 values except $\gamma_2 = 2.5$.

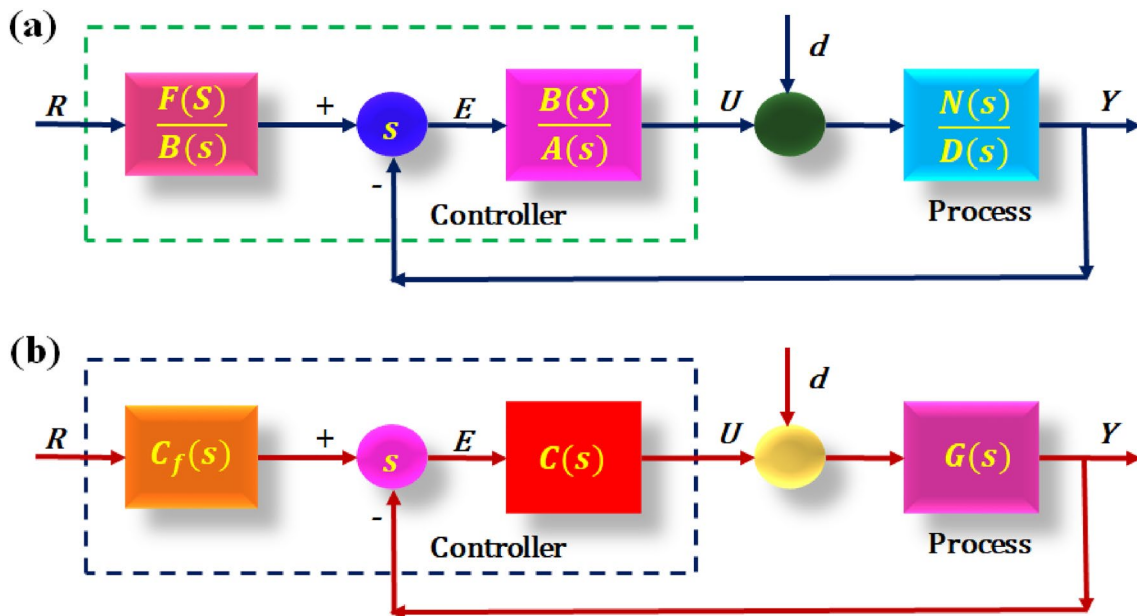


Fig. 5 Block diagram of a equivalent CDM controller b polynomial CD-PIC system

Fig. 6 Graphical representation of Servo responses **a** Group-I and **b** Group-II

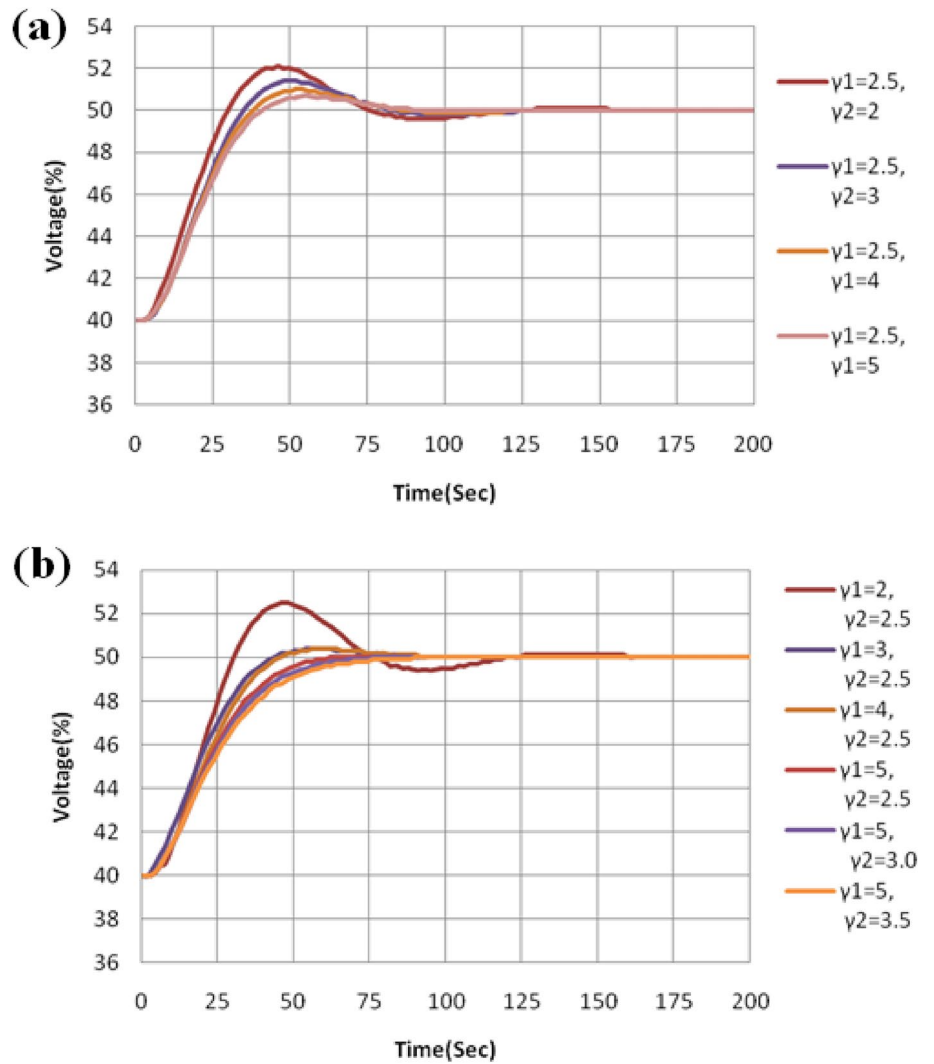


Table 1 Summarization of the effect of stability indices on CD-PIC performance

Group	γ_1	γ_2	ISE	IAE	SS error	t_r (sec)	t_s (sec)	OS (%)
I	2.5	2	3.089	11.49	0	31	170	20
	2.5	3	3.057	10.69	0	36	130	13.33
	2.5	4	3.071	10.32	0	38	84	8.89
	2.5	5	3.102	10.16	0	40	88	6
II	2	2.5	3.132	12.06	0	32	180	24.44
	3	2.5	3.062	10.44	0	36	90	11.11
	4	2.5	3.157	10.14	0	44	92	4.44
	5	2.5	3.312	10.66	0	62	62	0
	5	3	3.396	11.17	0	74	74	0
	5	3.5	3.478	11.73	0	80	80	0

*ISE: Integral Square Error, IAE: Integral Absolute Error, SS error: Steady State error; t_r : Rise time, t_s : Settling time, OS: Percentage Peak Overshoot (%)

The above-said analysis details the selection and influence of stability indices values γ_1 and γ_2 based on the closed-loop response of DMFC. From this analysis, a smooth, rapid response with minimum error values and impeccable time domain values are obtained for a CD-PIC with the value of stability indices $\gamma_1 = 5$ and $\gamma_2 = 2.5$ than other γ_1, γ_2 combinations.

Development of Coefficient Diagram Based PI Controller

In existing CDM-PI controller design, the designer is forced to specify the stability indices values. If the values specified does not offer the desired result, the controller design process has to be repeated which is hard and time consuming. To overcome the above difficulties, the CD-PIC proposed here gives the designer the freedom to choose the stability index values according to the transient response required which is considered to be advantage. Further, a fixed PI controller design with best stability index value is proposed which is considered to be a major difference.

The chosen CD-PIC polynomials are $A(s) = s$ and $B(s) = k_1 s + k_0$. The stability indices, $\gamma_1 = 5, \gamma_2 = 2.5$ were chosen for the CD-PIC strategy design. The stability indices (γ_i) and the equivalent time constant (τ) are used to derive the target characteristic polynomial which is given as $P_{Target}(s)$.

$$P_{Target}(s) = 0.0034s^3 + 0.0428s^2 + 0.214s + 0.214 \quad (10)$$

When a process is said to have small time constant, the transient response is found to exhibit large overshoot. By choosing the smaller time constant, the performance of the controller in reducing the overshoot is tested and the results show that the proposed controller reduces the overshoot to large extent when compared to other control strategies.

The characteristic polynomial equation above is used to calculate the CD-PIC polynomials, k_1 and k_0 , which are $k_1 = 13.407$ and $k_0 = 1$.

Calculations of CD-PIC attributes by comparing CD-PIC polynomials with the transfer function of a traditional PI controller.

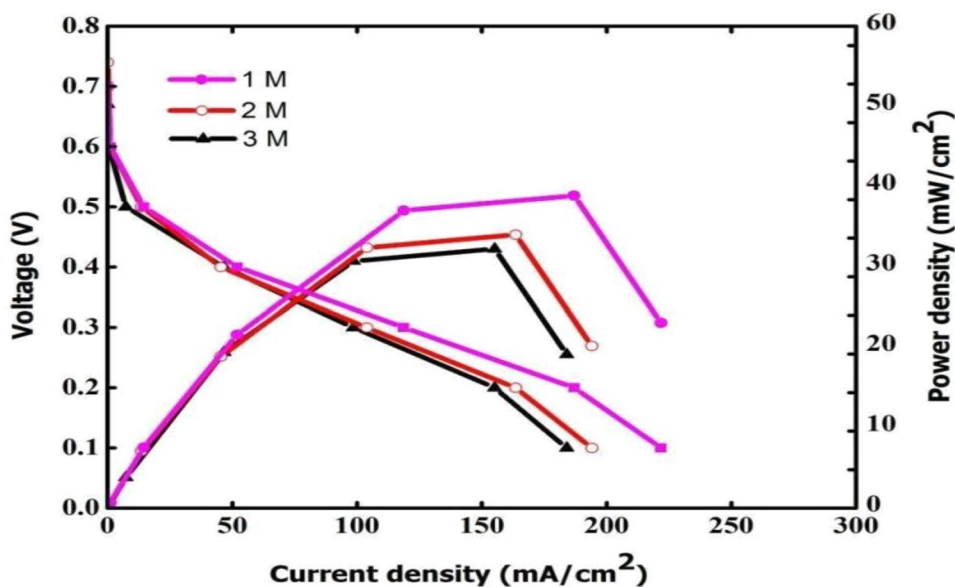
$$G_c(s) = \frac{B(s)}{A(s)} = K_c \left(1 + \frac{1}{T_i s} \right) = 13.407 \left(1 + \frac{1}{13.407s} \right) \quad (11)$$

$C_f(s)$ is derived from CD-PIC parameters without any extra calculations. It is represented in Eq. 12.

$$C_f(s) = \frac{F(s)}{B(s)} = \frac{k_0}{k_1 s + k_0} = \frac{1}{T_i s + 1} = \frac{1}{13.407s + 1} \quad (12)$$

The designed CD-PIC is used to develop a DMFC closed-loop system [34, 35]. In DMFC, experiments on load disturbance rejection and set point tracking are carried out. The proposed CD-PIC is applicable only when the transfer function model of the process to be controlled is available. Further, the model should be of first order plus time delay.

Fig. 7 Effects of the methanol concentration during DMFC performance



Results and Discussion

Impact of the Methanol Concentrations on DMFC Performance

The influence of the different methanol concentrations (1 M, 2 M, and 3 M) on the performance of DMFCs with 1 ccm of methanol flow rate is shown in Fig. 7. The cell performance with 1 M, 2 M, and 3 M methanol concentration was achieved a peak power density of 40 mW/cm², 35 mW/cm² and 32 mW/cm². Increases in the methanol concentration increase the methanol crossover could result in the difference the performance. The outcomes of the study concur that the ideal methanol concentration could be 1 M

methanol solution. Further closed-loop dynamic studies are conducted in direct methanol fuel cell with 1 M methanol concentration.

Characterization of Model-Based New Controller

The recently created Coefficient Diagram PI Controller was implemented in DMFC operation through simulation in the MATLAB platform. Outputs of CD-PIC were evaluated at different Operating Points (OP). In all the cases, Controller Progress Measuring Indices (CPM Indices) namely error indices [Integrated Square Error (ISE), Integrated Absolute Error (IAE)] and time domain indices [Rise time (t_r), settling time (t_s) and percentage maximum overshoot (%OS)] were determined [36] in addition to time versus cell voltage plots.

Fig. 8 Servo responses of set point monitoring at **a** 40% OP and **b** 60% OP

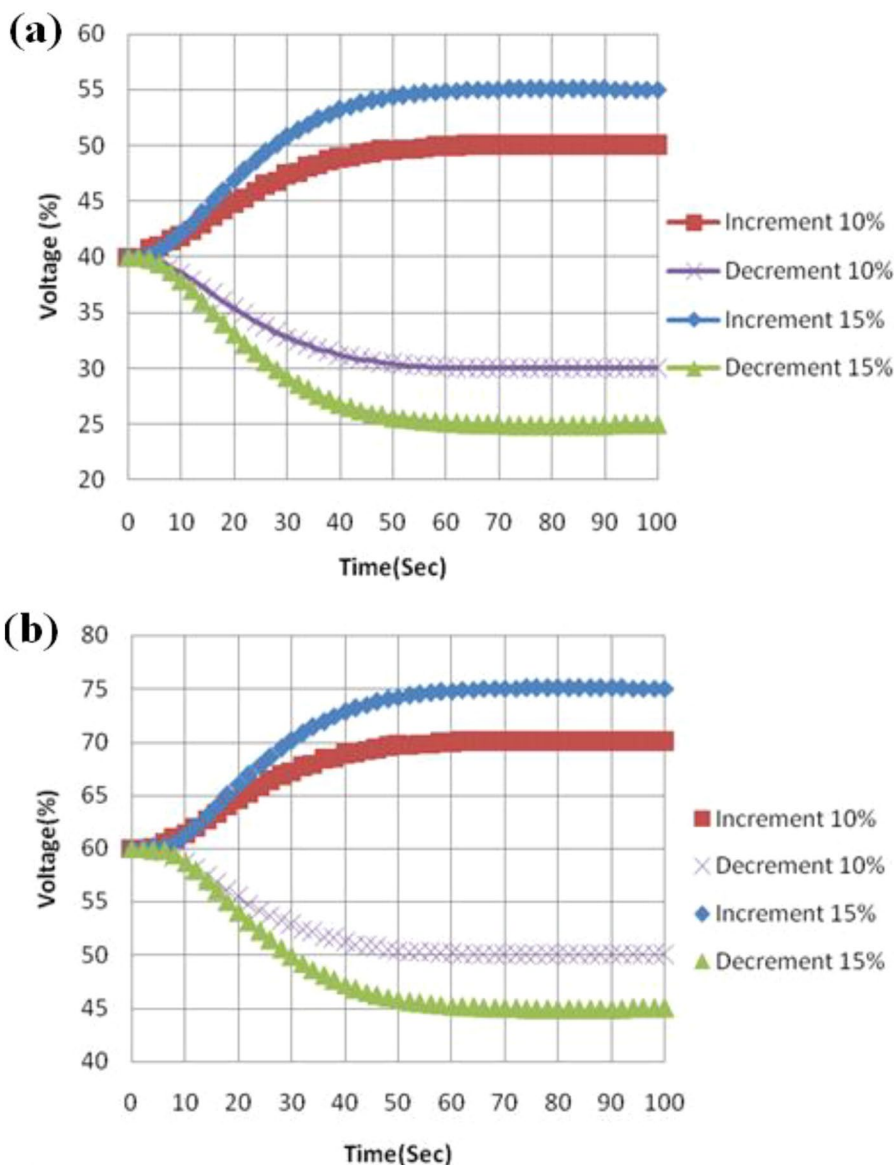
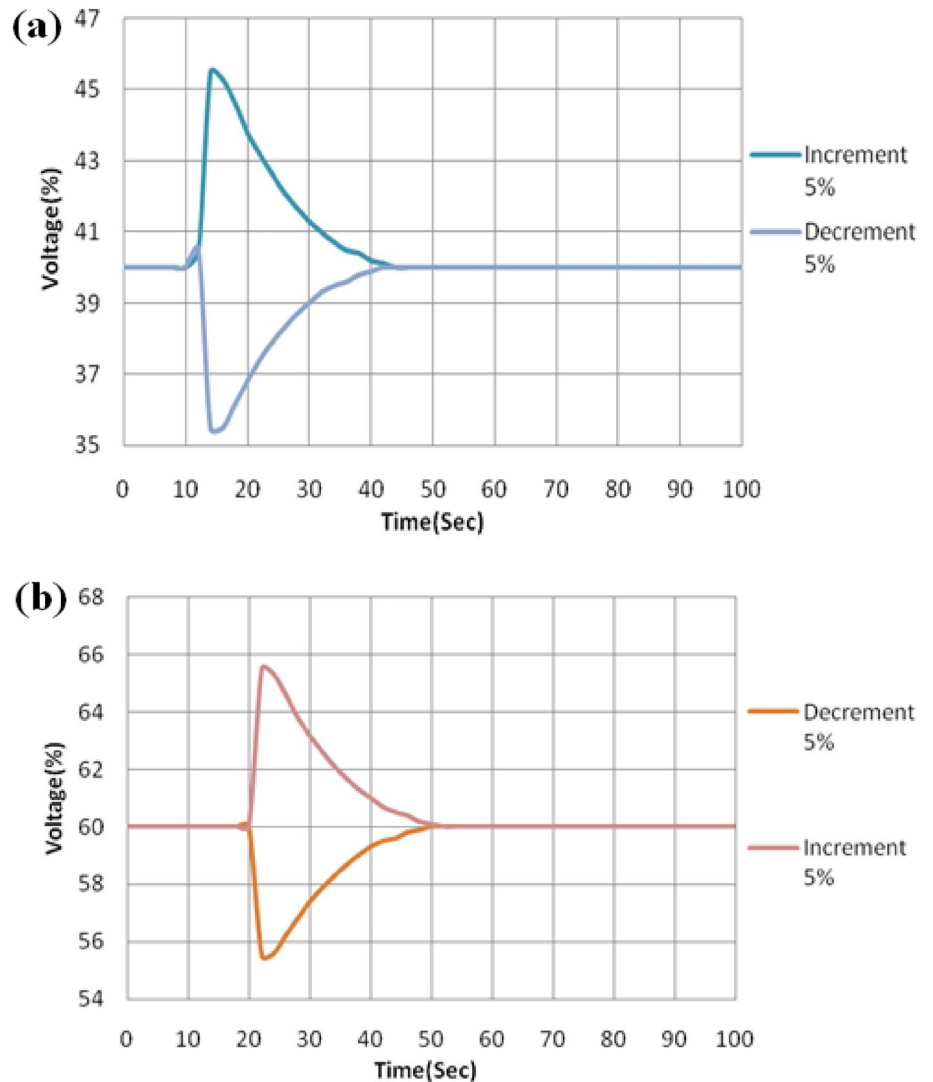


Table 2 Tabulation of parameters related to controller progress measuring indices

Step change (%)	Set point tracking: 40% OP					Set point tracking: 60% OP				
	Error indices		Time domain indices			Error indices		Time domain indices		
	ISE	IAE	t_r (sec)	t_s (sec)	% OS	ISE	IAE	t_r (sec)	t_s (sec)	% OS
+10 V	3.168	10.64	66	66	0	3.463	11.14	56	56	0
+15 V	3.17	10.78	58	58	0	3.465	11.26	62	62	0
-10 V	3.168	10.64	66	66	0	3.463	11.14	56	56	0
-15 V	3.17	10.78	58	58	0	3.465	11.26	62	62	0

Fig. 9 Servo responses of load rejection test at **a** 40% OP and **b** 60% OP



Set Point Monitoring and Load Abandonment Test

A closed loop run of CD-PIC with DMFC was done for set point changes and load variations. A step change of $\pm 10\%$ step size and $\pm 15\%$ step size at the OP of 40% cell voltage

were given in setpoint. At a different operating point, 60% of the set point’s cell voltage was reached again. Set point monitoring responses at both the functioning parameters are displayed in Fig. 8a and b. The performance evaluations are recorded in Table 2.

At 40% and 60% cell voltage operating points, the load abandonment responses of CD-PIC with DMFC are achieved for load variations of $\pm 5\%$. The performance is recorded as the load rejection responses of CD-PIC with DMFC are obtained for the load changes of $\pm 5\%$ at the operating points of 40% cell voltage and repeated at the operating point of 60% cell voltage. The recording of the performance is presented in Fig. 9a and b. It is found from the performance measures that the load rejection behavior of CD-PIC is almost same in 40% and 60% of the cell voltage at the Operating Parameters.

From Fig. 8a and b (CD-PIC set point tracking at 40% cell voltage and 60% cell voltage), it's clear that the action of CD-PIC has no overshoot and results in less settling time and no oscillations. This statement is confirmed by the CPM Indices given in Table 2. It is concluded from the above results that the proposed CD-PIC is effective in tackling the set point changes and brings the desired voltage faster and more smoothly. It is also proved from Fig. 9a and b, that the CD-PIC is also effective for load changes in DMFC operation.

Comparison of CD PIC Controller Settings with Conventional PIC Settings

A simulation run is carried out with Polynomial CD-PIC in the DMFC system at 40% set value of voltage. Similar studies are repeated in the same set value of voltage with the widely used conventional tuning rules-based PI controller settings Viz., Padmashree Chidambaram Tuning Rule (PCTR) [37], Ziegler & Nichols Tuning Rule (ZNTR) [38], Astrom and Hagglund Tuning Rule (AHTR) [39], Abdulla Awouda-Rosbi Bin Mamat Tuning Rule (ARTR) [40]. Servo responses of these tuning rules-based controllers along with CD-PIC (CDTR-Coefficient Diagram Tuning Rule) servo response are plotted in Fig. 10a. In addition, error signal analysis and control signal analysis of all PI Controllers are recorded and represented in Fig. 10b and c, which indicates that the Polynomial CD-PIC lowers the error level closer to zero rapidly [41]. Considering the results in Table 3 and the pictures below, it can be said that the suggested Polynomial CD-PIC outperforms the other conventional tuning techniques.

CD-PIC: Robustness in Setpoint Changes and Load Changes

To verify the endurance of the suggested coefficient schematic-based PIC, a closed loop simulation run is performed with step changes of $\pm 10\%$ and $\pm 15\%$ step sizes at the operating parameter of 30% cell voltage. Figure 11a displays the generated set point monitoring feedback, while Table 4 records the CPM Indices of CD-PIC. Apart from the set point monitoring examination, load abandonment experiments are also carried out at the same operating points of 30% cell voltage, with load variations of $\pm 10\%$ and $\pm 15\%$ (voltage) [42]. Figure 11b displays the reactions to the load rejection. Figure 11a and b, Table 4 clearly show how reliable the suggested CD-based-PI controller is found to be robust.

Conclusion

The impact of the various methanol concentrations on the progress of DMFC was analyzed. The cell performance with 1.0 M, 2 M, and 3 M methanol concentration was achieved with a peak power density of 40 mW/cm², 35 mW/cm², and 32 mW/cm². Increases in the methanol concentration increase the methanol crossover could result in the difference of performance. The outcomes of the tests concur that the ideal concentration of methanol could be 1 M methanol solution. Further closed-loop dynamic studies are conducted in DMFC with 1 M methanol concentration. A new CD-PIC for DMFC operation is proposed and tested through simulation. The CD-PIC is easy to design with the fixed stability index values and the fixed PI tuning rules. Based on the simulation results, the performances of the proposed CD-PIC are evaluated under set point monitoring and load abandonment tests. Based on the analysis, it is found that CD-PIC yields lower error values and fast settling time. To validate the results of CD-PIC, the performances of the CD-PIC were compared with performances of widely used tuning rules-based PI. A robustness test of the CD-PIC is also conducted to support its performances using set point monitoring and load abandonment test. The analysis includes step changes in set point and load change values $\pm 10\%$ and $\pm 15\%$ for cell

Fig. 10 Comparison of CD controller settings analysis with conventional controller during **a** servo response, **b** error signal and **c** control signals

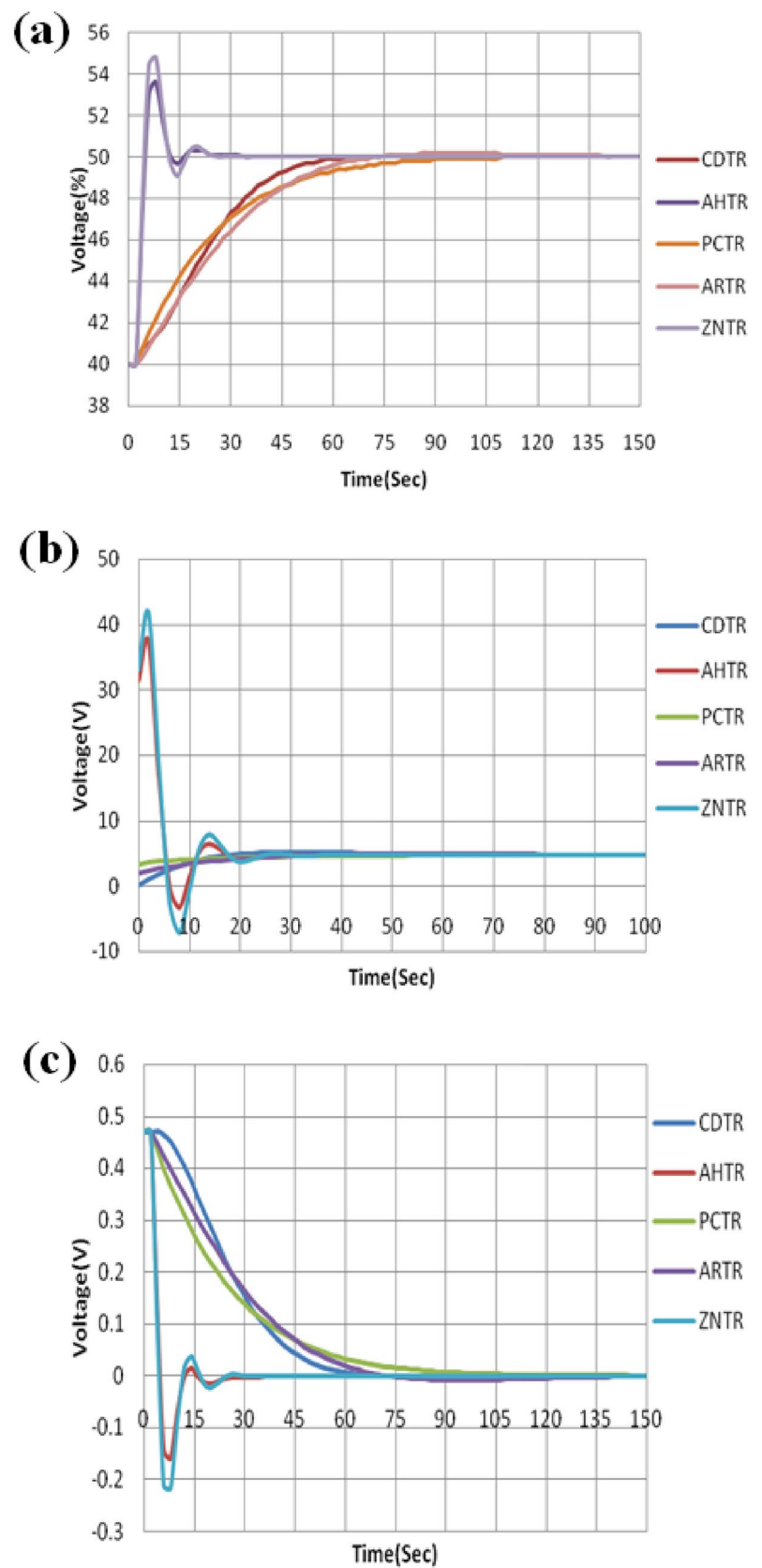


Table 3 Evaluation of error and time indices at 40% OP during the changes of controller settings

Rule	Error indices		Time domain indices		
	ISE	IAE	t_r (s)	t_{rs} (s)	OS (%)
CDTR	3.168	10.64	66	66	0
ZNTR	0.706	2.61	4.5	28	9.6
AHTR	0.638	2.34	5	36	7.2
PCTR	2.636	10.98	112	112	0
ARTR	3.118	11.85	73	112	4

voltage at the OP of 30% and 70%, respectively. The results reveal that the designed CDM-PIC is found as highly robust. According to the findings, the polynomial CD-PIC provides outstanding performance. The proposed control scheme can be most suitable for similar types of processes.

Fig. 11 Graphical representation of **a** set point tracking test at 30% OP and **b** load rejection test at 30% OP

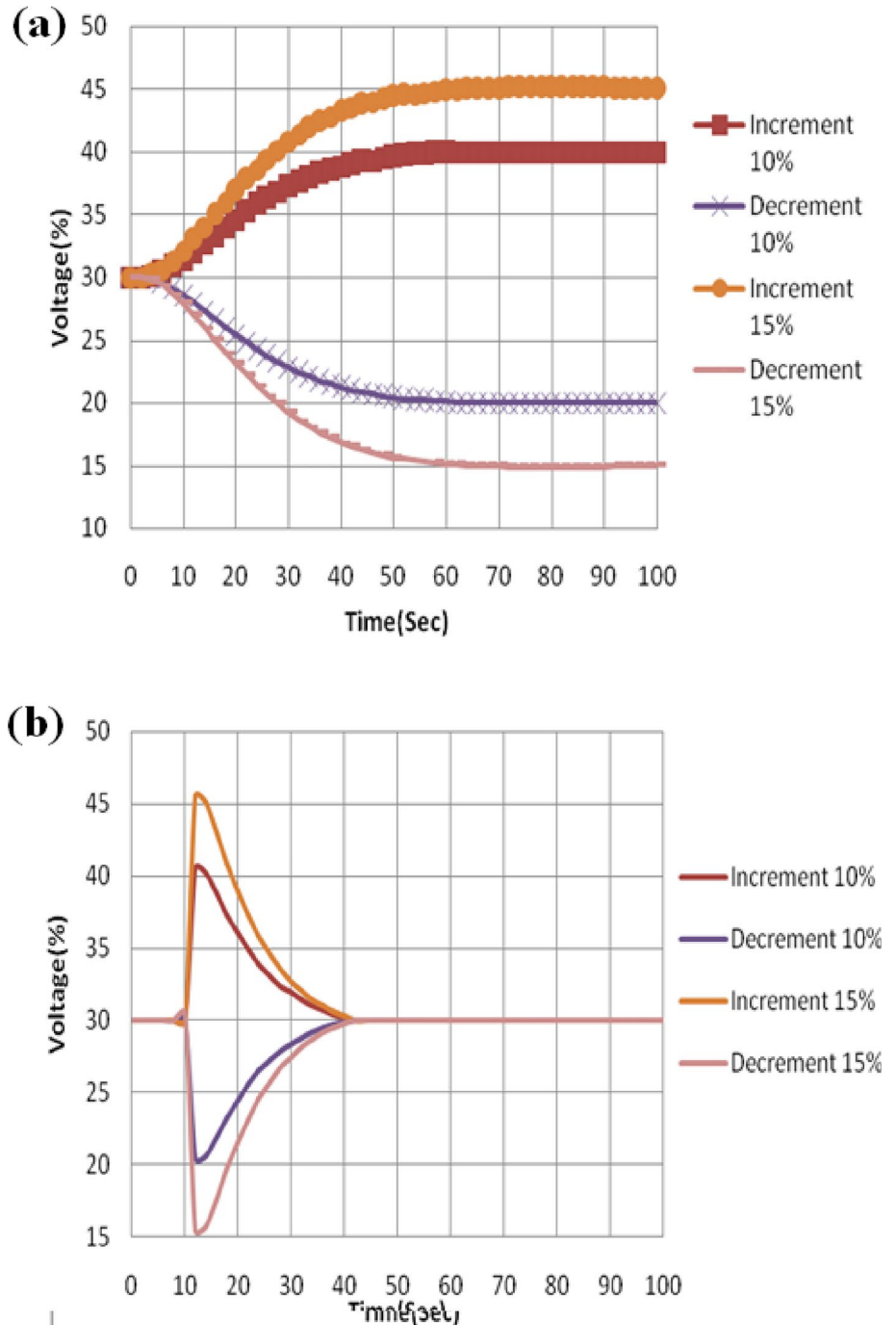


Table 4 Records of the CPM Indices of CD-PIC during servo and load robustness

Step change (%)	Servo robustness: 30% OP					Load robustness: 30% OP				
	Error indices		Time domain indices			Error indices		Time domain indices		
	ISE	IAE	t_r (sec)	t_s (sec)	OS %	ISE	IAE	t_r (sec)	t_s (sec)	OS %
+ 10 V	3.026	10.43	58	58	0	0.782	5.96	53	53	0
+ 15 V	3.028	10.55	60	60	0	0.783	6.02	56	56	0
- 10 V	3.026	10.43	58	58	0	0.782	5.949	53	53	0
- 15 V	3.028	10.55	60	60	0	0.783	6.009	56	56	0

Acknowledgements This work was supported by the National Research Foundation of Korea (NRF) grant funded by the Korea government (MSIT) (No. 2021R1A2C2006888), and grant received under the Research Promotion Scheme of AICTE, New Delhi, India.

Data availability Data will be made available on request.

Declarations

Conflict of interest The authors declare that they have no known competing financial interests or personal relationships that could have appeared to influence the work reported in this paper.

References

1. A. Pramuanjaroenkij, S. Kakaç, *Int. J. Hydrogen Energy* **48**, 9401–9425 (2023)
2. Z. Wang, Z. Liu, L. Fan, Q. Du, K. Jiao, *Energy Rev.* **2**, 100017 (2023)
3. M. Mehregan, S.M. Miri, S.M. Hashemian, M.M. Balakheli, A. Amini, *Korean J. Chem. Eng.* **40**, 1340 (2023)
4. M. Boni, S.S. Rao, G.N. Srinivasulu, *Korean J. Chem. Eng.* **39**, 116 (2022)
5. N. Sazali, W.N. Wan-Salleh, A.S. Jamaludin, M.N. Mhd-Razali, *Membranes* **10**, 99 (2020)
6. M.A.U. Din, M. Idrees, S. Jamil, S. Irfan, G. Nazir, M.A. Mudasir, R. Saidur, *J. Energy Chem.* **77**, 499 (2023)
7. L. Yaqoob, T. Noor, N. Iqbal, *Int. J. Energy Res.* **45**, 6550 (2021)
8. S.H. Woo, S. Kim, S. Woo, S.H. Park, Y.S. Kang, N. Jung, S.D. Yim, *Korean J. Chem. Eng.* **40**, 2455 (2023)
9. M.A.A. Khalid, N. Abdullah, M.N.M. Ibrahim, R.M. Taib, S.J.M. Rosid, N.M. Shukri, W.N.B.W. Abdullah, *Korean J. Chem. Eng.* **39**, 1487 (2022)
10. F. Zenith, U. Krewer, *J. Process. Control.* **20**, 630 (2010)
11. S. Manabe, *IFAC Proc. Vol.* **31**, 211 (1998)
12. Y.L. Ouyang, C.S. Chiu, J.L. Li, G.C. Hsieh, *IEEE International Conference on Fuzzy Systems*, p. 1 (2012).
13. Q. Yang, B. Gao, Q. Cheng, G. Xiao, M. Meng, *M. Energy* **238**, 121710 (2021)
14. J.P. Coelho, T.M. Pinho, J. Boaventura-Cunha, *Arab. J. Sci. Eng.* **41**, 3663 (2016)
15. S.E. Hamamci, P.K. Bhaba, S. Somasundaram, T. Karunanithi, In *Proceedings of TIMA*, p. 145 (2007)
16. A.S. Arico, S. Srinivasan, V. Antonucci, *Fuel cells* **1**, 133 (2001)
17. Y.C. Kim, S. Manabe, *IFAC Proc. Vol.* **34**, 147 (2001)
18. B. Meenakshipriya, K. Kalpana, *IFAC Proc. Vol.* **47**, 620 (2014)
19. X. Chi, F. Chen, T. Mo, Y. Li, B. Wu, In *2023 13th International Conference on Power, Energy and Electrical Engineering*, p. 364 (2023)
20. R. Govindarasu, S. Somasundaram, *Processes* **8**, 353 (2020)
21. E. Giordano, A. Zaffora, L. Iannucci, M. Santamaria, S. Grassini, In *IEEE International Instrumentation and Measurement Technology Conference (I2MTC)*, Kuala Lumpur, Malaysia, p. 1 (2023)
22. U. Krewer, K. Sundmacher, *J. Power. Sources* **154**, 153 (2005)
23. K.R. Sundaresan, C.C. Prasad, P.R. Krishnaswamy, *Ind. Eng. Chem. Process Design Develop.* **17**, 237 (1978)
24. P. Argyropoulos, K. Scott, W.M. Taama, *J. Power. Sources* **87**, 153 (2000)
25. R. Govindarasu, R. Parthiban, P.K. Bhaba, *Elixir Int. J. Chem. Eng.* **72**, 25428 (2014)
26. R. Govindarasu, S. Somasundaram, P.K. Bhaba, *Taga J. Graphic Tech.* **14**, 1525 (2018)
27. S. Manabe, In *Proceedings of the 4th Asian Control conference, Singapore*, p. 1161 (2002)
28. R. Govindarasu, R. Parthiban, P.K. Bhaba, *Int. J. Chem. Sci.* **12**, 1645 (2014)
29. W. Giernacki, T. Sadalla, *J. Control Eng. App. Inform.* **19**, 31 (2017)
30. B. Meenakshipriya, K. Saravanan, P. Kanthabhabha, S. Somasundaram, *J. Asian Sci. Res.* **5**, 78 (2012)
31. E. Imal, *J. Electr. Electron. Eng.* **9**, 1003 (2009)
32. S. Manabe, In *Proceedings of the 2nd Asian Control Conference, Seoul*, p. 135 (1997)
33. B. Meenakshipriya, K. Saravanan, K. Krishnamurthy, P.K. Bhaba, *J. Asian Sci. Res.* **5**, 78 (2012)
34. R. Rinu-Raj, L.D. Vijay-Anand, *Int. J. Theoret. Appl. Res. Mec. Eng.* **2**, 2319 (2013)
35. P.K. Bhaba, S. Somasundaram, *J. Sens. Transducer* **133**, 53 (2011)
36. U. Krewer, A. Kamat, K. Sundmacher, *J. Electroanal. Chem. Electroanal. Chem.* **609**, 105 (2007)
37. P. Padma-Sree, M.N. Srinivas, M. Chidambaram, *Comput. Chem. Eng.. Chem. Eng.* **28**, 2201 (2004)
38. D.R. Coughanowr, *Process system analysis and control*, 2nd edn. (McGraw-Hill, 1991), p.213
39. K.J. Astrom, T. Hagglund, *IFAC Control Eng. Pract.* **9**, 1163 (2001)
40. A.E.A. Awouda, R.B. Mamat, In *2010 The 2nd International conference on computer and automation engineering* **5**, 171 (2010)
41. A. O'dwyer, *Handbook of PI and PID controller tuning rules*, 2nd edn. (Imperial College Press, 2009)
42. Z. Hua, Z. Zheng, E. Pahon, M.C. Péra, F. Gao, *Energy Conv. Manag.* **231**, 113825 (2021)

Publisher's Note Springer Nature remains neutral with regard to jurisdictional claims in published maps and institutional affiliations.

Springer Nature or its licensor (e.g. a society or other partner) holds exclusive rights to this article under a publishing agreement with the author(s) or other rightsholder(s); author self-archiving of the accepted manuscript version of this article is solely governed by the terms of such publishing agreement and applicable law.